RESEARCH ARTICLE:

Examination of Balancing in a Real-World Inverted Pendulum

Laura Alvarez-Hidalgo[1*], & Ian S. Howard[1*]
[1] School of Computing, Engineering and Mathematics, University of Plymouth, Plymouth, Devon, United Kingdom.

[*]Correspondence should be addressed to: ISH: ian.howard@plymouth.ac.uk
Telephone: +44 1752 586324

Keywords: Human Balance, Inverted Pendulum, Predictive Control, Learning Transfer, Real-World Dynamics, Sensorimotor Control.

Number of pages: 17
Number of figures: 7
Number of tables: 2
Number of words for Abstract: 281
Number of words for Introduction: 531
Number of words for Discussion: 1033

Statement of Financial Interests or Conflicts of Interest

The authors declare that they have no financial, personal, or professional interests that could be construed to have influenced the paper.

Acknowledgements

Financial support for this project for LAH was provided by the Engineering and Physical Sciences Research Council (EPSRC) and the University of Plymouth. Financial support for ISH was provided by the University of Plymouth. During the preparation of this work, LAH and ISH utilized ChatGPT-5 for proofreading.

Abstract (281)

Motor adaptation is typically studied using simplified virtual tasks. Here, we investigated how humans learn to stabilize a physically unstable, underactuated system, and how participants cope with changes in the system's dynamics. Twelve right-handed adults balanced a real inverted pendulum by moving a cart along a linear rail. Study 1 characterized the passive mechanical properties of three pendulums (short, medium, and long) using free-oscillatory decay and fall to ±30° trials, after their release from the upright position. Longer rods exhibited slower decay and lower natural frequencies, as well as a longer duration before falling, indicating greater passive stability. Study 2 assessed human motor control of the pendulum to maintain balance. Human participants trained with the medium pendulum (30 trials) and were then tested with all three pendulums (20 trials each). During training, balance performance improved significantly, with time to

failure increasing over trials. During testing, performance scaled with pendulum length, and longer rods were easier to balance. Similar peak cart velocities were observed across conditions, suggesting equivalent actuation effort. Additionally, as expected, pendulum angular velocities decreased with rod length, reflecting underlying inertial differences. Pendulum passive dynamics closely matched behavioral performance, supporting a strong link between intrinsic system properties and balancing outcomes. These findings show that motor learning in physically unstable environments is not only shaped by feedback and effort, but also by the alignment of human control strategies and abilities with the natural dynamics of the plant. We note that in this study, we used a modified pendulum rig previously employed to examine control engineering approaches to modelling balance, thereby generating a dataset that can later be used to compare human performance with real-time computer control implementations of the same tasks.

Introduction (531)

Humans continually adjust their movements to meet changing environmental and task demands. This adaptive capability, also known as motor adaptation, relies on the nervous system updating internal models of the body and environment through sensory feedback and error-based learning (Shadmehr et al., 2010; Wolpert et al., 2011; Howard et al., 2013, 2017). These internal models support predictive control, enabling behavior to remain effective despite noise, delays, and perturbations.

Much of what is known about motor adaptation derives from tightly controlled laboratory tasks using artificial perturbations, such as visuomotor rotations or curl field force perturbations applied to the hand (Howard et al., 2009, 2012; Franklin and Wolpert, 2011; Krakauer and Mazzoni, 2011; Taylor and Ivry, 2012). While these paradigms afford clear experimental leverage on learning mechanisms, they often minimize or eliminate key properties of everyday interactions, such as the combined effects of mass, inertia, contact forces, and intrinsic instability, by, for example, mapping hand motion to a screen cursor or employing isometric contractions. Consequently, important questions remain about how humans adapt when confronted with the physical dynamics of real objects that differ in their intrinsic properties.

Balancing tasks offer an ecologically meaningful window onto such control problems. They are inherently unstable and demand the integration of feedback and predictive control to maintain equilibrium. The inverted pendulum is a system that captures core challenges of real-world control: underactuation, sensorimotor delays, and high sensitivity to small disturbances (Scott, 2004; Gawthrop and Wang, 2006; Liu and Todorov, 2007). Comparable dynamics arise in human posture, manual object manipulation, and everyday load handling (e.g., carrying a tray or a cup of tea), where success hinges on anticipating and counteracting the evolving effects of the object's dynamics.

Many previous studies have examined balance control using simplified or virtual implementations, such as tracking a simulated pendulum or stabilizing one via a robotic interface that abstracts away some mechanical complexities (Burdet et al., 2001; Mehta and Schaal, 2002; Milner and Franklin, 2005; Howard et al., 2009). These approaches help isolate specific mechanisms but often rely on artificially simulated sources of feedback and omit important aspects of the task.

The present study uses an authentic, physically real inverted pendulum task that preserves natural sensory cues. These include full-field visual information about the pendulum and require direct interaction with forces arising from the system's dynamics. Participants stabilized a real-world inverted pendulum by manually controlling a rolling cart in an underactuated setting, in which the rod is controlled only indirectly via base motion. Crucially, we varied pendulum length (short, medium, and long), thereby altering time constants and stability characteristics. This design allows us to quantify how human participants balance during different dynamic conditions.

We base the design of the experiments on a previous pendulum rig (Alvarez Hidalgo and Howard, 2022, 2024), developed to investigate control engineering approaches to balance, which can operate more effectively than human performance. However, in the future, we envisage that the same setup will be used to test more biologically realistic computational models that incorporate sensory and motor delays, as well as sensor and actuation noise, so that the actual human performance and behavior identified in this study can be compared with the results of simulations and examined further.

Methods

Participants

Twelve right-handed adults (eight female, four male) participated in the study. Participants were randomly assigned to one of two groups (Group A or Group B) to counterbalance the order of experimental conditions. Group A included three females (mean age: 22.16 ± 1.22 years) and three males (27.59 ± 0.86 years), while Group B comprised five females (23.56 ± 2.11 years) and one male (28.99 ± 0.00 years). This between-subjects counterbalancing strategy ensured that any order-related effects were evenly distributed across conditions.

All participants were naïve to the purpose of the study and provided written informed consent prior to participation. Handedness was confirmed using the Edinburgh Handedness Inventory (Oldfield, 1971), verifying that all participants were right-handed. The study received ethical approval from the Faculty Research Ethics and Integrity Committee at the University of Plymouth and was conducted in accordance with institutional guidelines.

Apparatus

The experimental task was implemented using a custom-built inverted pendulum apparatus mounted on a standard-height desk (Figure 1), very similar to that described in prior work (Alvarez Hidalgo and Howard, 2022, 2024). The system consisted of a rigid horizontal frame supporting a rolling cart that moved along the X-axis. A detachable vertical rod was affixed to the cart via a pivot joint, forming an underactuated inverted pendulum.

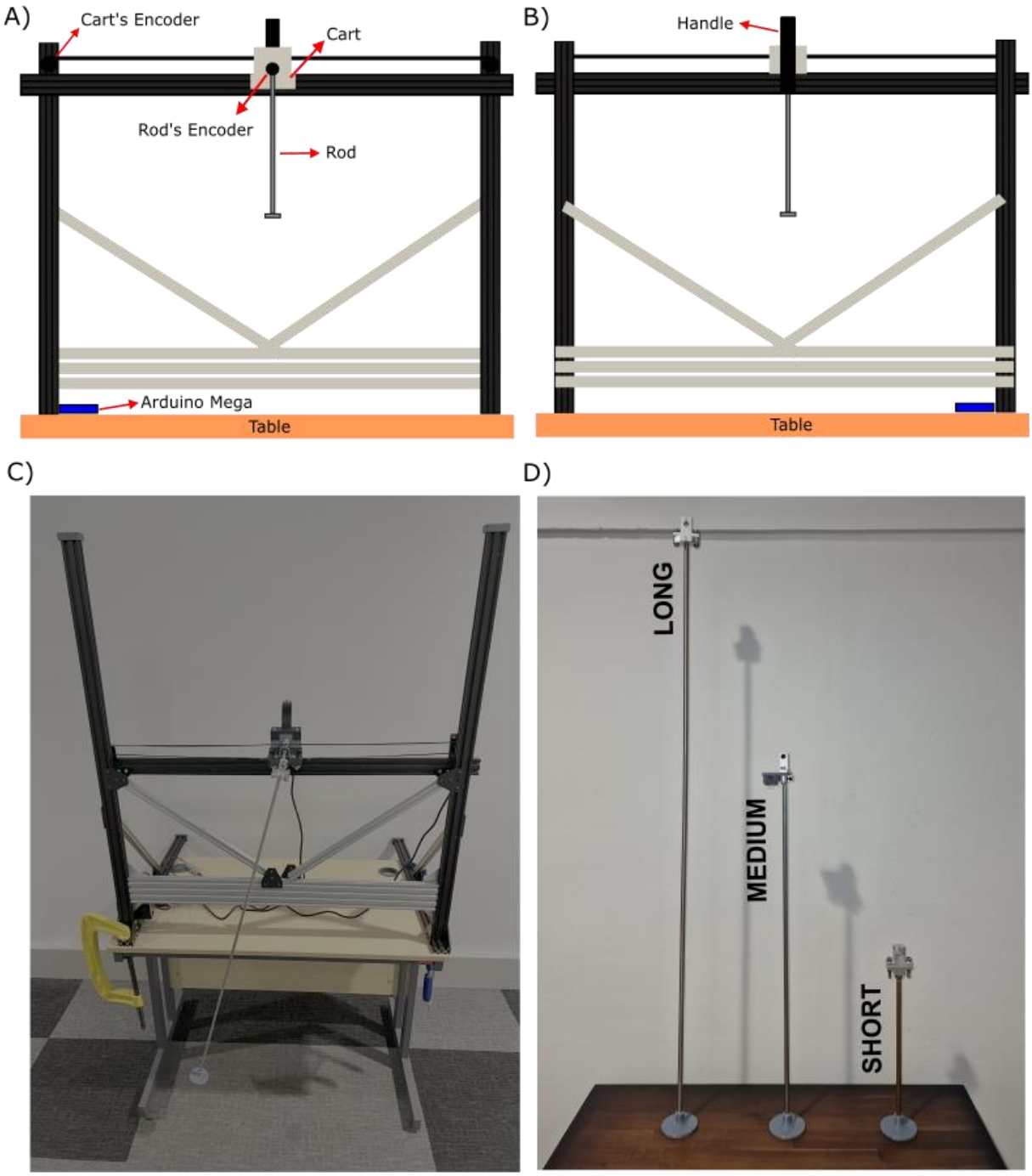

Figure 1. Schematic and photographic views of the inverted pendulum apparatus. **A)** Front view of the setup, showing the rolling cart and vertical rod assembly. **B)** Rear view, highlighting the handle used for manual control. **C)** Photograph of the complete rig mounted on a standard-height desk. **D)** The three interchangeable pendulum rods (short, medium, and long).

Motion data were recorded using two rotary encoders (2400 pulses per revolution, using all waveform edges). One encoder was mounted at the end of the rail and measured the

horizontal displacement of the cart. The second encoder was located at the rod-cart pivot and tracked its angular displacement relative to the vertical. To systematically vary the pendulum dynamics, three rods of different lengths were used: a short brass rod (305 mm, 90 g), a medium stainless-steel rod (635 mm, 143 g), and a long stainless-steel rod (1030 mm, 216 g). All rods shared the same 8 mm diameter and mounting interface to ensure consistent mechanical coupling with the cart.

Table 1. Mechanical properties of the three inverted pendulum rods.

		Short Pendulum	Medium Pendulum	Long Pendulum
Length (L)	[m]	0.305	0.635	1.030
Mass (m)	[Kg]	0.090	0.143	0.216
Length to CoG	[m]	0.153	0.318	0.515
Weight (W)	[N]	0.883	1.403	2.119
Estimated MoI (I)	[$Kg \cdot m^2$]	0.003	0.019	0.076

Participants controlled the cart's position via a rear-mounted handle attached to the cart. The entire rig was securely clamped to the desk to maintain mechanical stability. An Arduino Mega 2560 microcontroller provided real-time data logging of pendulum angle and cart position, at a rate of approximately 10 Hz, with each measurement recorded with an associated precise timestamp. Interpolation was then carried out to provide measurement samples at precisely 100 Hz. The pendulum apparatus was ergonomically configured to ensure consistent access and comfort across participants.

Experimental Setup

Two complementary studies used the same inverted-pendulum apparatus (Figure 1). Auditory tones cued the start and stop of a trial. Study 1 quantified passive mechanical dynamics without human control input. Study 2 examined human balance control while participants attempted to stabilize the inherently unstable inverted pendulum. Uncontrolled and controlled trial termination thresholds were identical across studies. In both cases trials terminated when the pendulum exceeded ±30°.

Study 1: Passive System Identification

To better understand the dynamical properties of the inverted pendulum system, we conducted a set of trials without human control. These characterization trials were designed to capture the passive dynamics of the system and to quantify how each pendulum length affected stability and oscillatory decay behavior. For each pendulum length, we recorded data using two passive protocols.

The first protocol examined uncontrolled full decay, and a single trial for each pendulum length was recorded. In this protocol, the rod was released from the upright position and

allowed to oscillate until motion ceased, yielding a continuous decay trajectory. We note here that the upright position corresponded to 180° and decayed towards 0°.

The second protocol used an uncontrolled 30° fall. In this case, the rod was manually raised to its upright position (here defined at 0°) and released to fall freely. The trial ended when the pendulum angle reached ±30°. This limit was also used in Study 2. To get a good estimate of the effect of the pendulum dynamics, 20 trials were collected per length.

We note that there was always variability in setting up the experiment (angle and velocity), as this was a noisy process, and there were also random disturbances of the rod from the environment (such as from air currents).

Study 2: Human Study of Balance

Prior to the start of the human experiments, participants were instructed to move the cart left and right while holding the handle of the experimental rig. They were also told to focus their gaze exclusively on the top of the rod throughout the trials. Additionally, they were instructed to begin moving upon hearing a “beep”, and to stop moving upon hearing a second “beep.”

During each trial, participants held the handle attached to the cart. Once a participant was set up and ready, the researcher slowly raised the pendulum rod towards 180° from its initial resting position. When the rod's encoder detected that the angular velocity had dropped below 5 $\mathrm{deg \cdot s^{-1}}$ and the position was at 180°, a 3 second auditory tone (400 Hz) was played. Then, the encoder count was reset to zero, defining the upright position of the pendulum as 0°, which was the reference point for the experiment.

Participants then attempted to balance the inverted pendulum. Each trial ended either when the rod angle exceeded ±30°, or when the participant successfully maintained balance for 10 seconds. At the conclusion of each trial, another 3 second auditory tone was played to signal to both the participant and the researcher that the trial had ended.

Participants did not receive any formal feedback on their performance, aside from being able to observe how long they had balanced the pendulum. No scheduled breaks were provided during the experiment, apart from the brief pauses between trials. Participants also rested briefly during changes in pendulum length.

Each participant completed one training phase followed by three testing phases, one for each rod length (Figure 2). During the training phase, participants always used the medium-length inverted pendulum and completed a total of 30 trials.

After training, participants proceeded to the testing phase, beginning with 20 trials using the same medium-length rod. They then completed 20 trials with each of the remaining two rod lengths: the short and the long sized inverted pendulum. The order in which participants performed the short and long rod testing phases was counterbalanced across participants to control for potential order effects.

Each testing phase consisted of 20 consecutive trials using a single rod length. In total, each participant completed 90 trials: 30 during the training phase and 60 during the testing

phases (20 per rod length). The entire experiment took approximately 60 minutes to complete per participant.

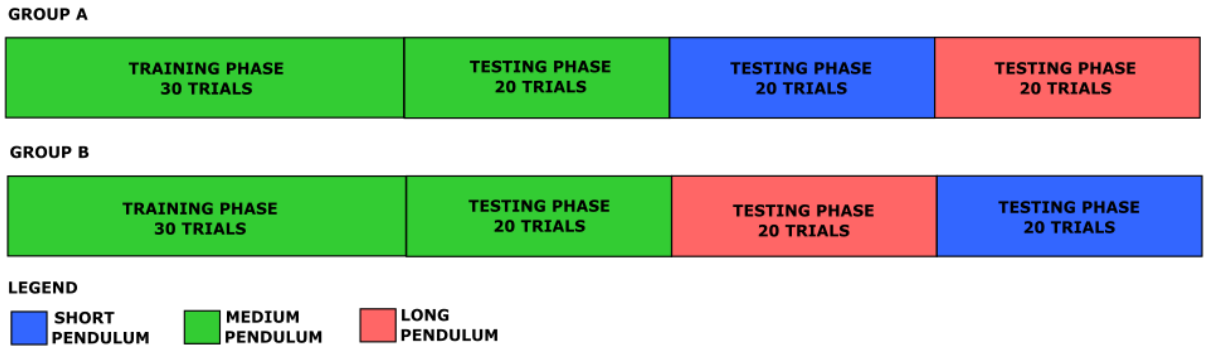

Figure 2. Experimental design and trial structure across conditions. Each row shows the sequence of phases for each group. All participants trained with the medium rod (30 trials; green), then completed testing phases (20 trials each) with the short (blue), medium (green), and long (red) rods.

Measurements

The rotary encoders provided continuous, time-indexed measurements of the cart motion and the pendulum angle. Cart position x(t) was obtained from an encoder coupled via a timing pulley and expressed as an angular-equivalent displacement (°) for consistency with downstream velocity measures. Pendulum angle θ(t) was recorded at the pivot encoder and zeroed at the upright position, such that θ = 0º denotes the unstable equilibrium.

Rod-Specific Mechanical Parameters

To characterize the pendulums, the following mechanical properties were measured or calculated:

Length (L): Distance from pivot to tip in meters.

Mass (m): Measured using a balance in Kg.

Centre of Gravity (CoG): The point where the rod's weight effectively acts. This was assumed to be at half the length of the rod.

$$CoG = \frac{L}{2} \tag{1}$$

Moment of Inertia (I): A measure of the rod's resistance to angular acceleration about its end point, in kg·m^2.

$$I = \frac{1}{3}\, m \cdot L^2 \tag{2}$$

Weight (W): The gravitational force acting on a body's mass, in Newtons.

$$W = m \cdot g \tag{3}$$

These parameters can be used to derive linearized dynamics about the upright equilibrium point. The small-angle natural frequency of the inverted pendulum model is:

$$f_n\,(t) = \frac{1}{2\pi}\sqrt{\frac{mgl}{CoG + ml^2}} \tag{4}$$

which we used to characterize the pendulum dynamics in the passive trials (Study 1).

Angle-based kinematics

To characterize the angle-based kinematics of our system, the angle and angular velocity for the cart position and pendulum angle were calculated. Angular velocity at the cart encoder ($\dot{\theta}_{Cart}$) and angular pendulum velocity ($\dot{\theta}_{Pend}$) were obtained by numerically differentiating the encoder-measured pendulum angle after converting counts to angle and correcting for wraparound.

$$\dot{\theta}_{Cart}\,(t) = \frac{d\theta_{Cart}(t)}{dt} \tag{4}$$

$$\dot{\theta}_{Pend}\,(t) = \frac{d\theta_{Pend}(t)}{dt} \tag{5}$$

Outcome measures aligned to Results

Time to failure was defined as the duration from the start of the trial to termination. Trials ended either when the absolute value of the pendulum angle exceeded 30°, or when the participant successfully maintained balance for a maximum of 10 seconds. This measure reflects the participant's ability to stabilize the system over time.

$$t_{30} = t_{end} - t_{start} \tag{6}$$

Peak angular velocity refers to the maximum absolute speed at the respective encoder attained during each trial. The peak angular velocity from the cart position encoder was related to the maximum instantaneous control effort. For group summaries in the Results section, we focused on the last 10% of trials within each phase/condition to evaluate final performance and compute mean values for each participant.

Natural frequency f_n is the intrinsic (undamped) oscillation rate of the linearized pendulum about the inverted equilibrium.

Results

This section covers the dynamic properties of the pendulum system and the behavioral outcomes across both passive and active balancing conditions. We first describe the findings from Study 1, which quantified passive decay and fall dynamics in the absence of human control. We then present the main behavioral results from Study 2, including

changes in time to failure across training and testing phases, as well as peak velocity metrics for both the cart and pendulum. Where appropriate, statistical comparisons are based on repeated-measures ANOVAs with post hoc corrections, and all reported effects are accompanied by descriptive statistics and standard error estimates.

Study 1: Passive System Identification

Free Decay

Total decay time from vertical release increased monotonically with rod length. The short rod reached near-zero motion after 100.09 s, while the medium rod decayed after 240.08 s, and the long rod took approximately 300.10 s to settle. These durations reflect the increasing moment of inertia and the smaller relative effect of the restoring torque associated with longer pendulums, which prolong the time required for energy dissipation in the absence of external control.

The oscillation frequency exhibited the inverse pattern, indicating that longer pendulums exhibit slower passive dynamics: the long pendulum oscillated at 0.59 Hz (period = 1.71 s), the medium at 0.74 Hz (period = 1.35 s), and the short at 1.05 Hz (period = 0.95 s). Figure 3 shows single-trial decay durations and representative angular trajectories for each condition.

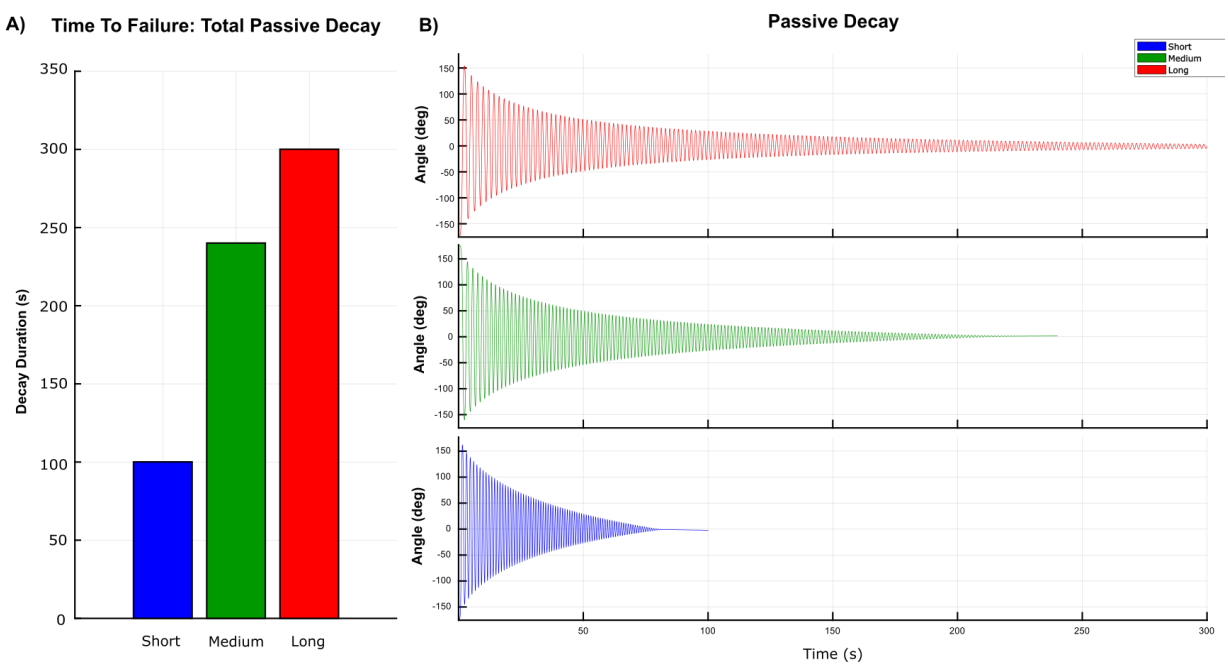

Figure 3. Passive free-decay dynamics for the three rod lengths. **A)** Overall decay time per rod length. **B)** Angular pendulum trajectories as a function of time for the unassisted free-decay experiments.

Fall to ±30 degrees

Fall time from upright to reach the ±30° threshold increased consistently with rod length, again in line with the slowing down of passive dynamics as pendulum length increased.

To evaluate the effect of pendulum length on passive fall behavior, a one-way repeated-measures ANOVA was conducted on the time to failure across three conditions: short, medium, and long pendulums. Each trial was terminated when the pendulum reached an angular displacement of ±30°, marking the loss of balance under passive dynamics.

A one-way repeated-measures ANOVA on passive time to failure showed a main effect of condition, $F(2, 57) = 5.78$, $p = 0.005$, $\omega^2 = 0.137$. Pairwise post-hoc comparisons with Bonferroni correction showed that the short pendulum yielded significantly shorter times to failure compared to both medium ($p_{bonf} = 0.046$) and long ($p_{bonf} = 0.006$). No significant difference was observed between the medium and long conditions ($p_{bonf} = 1.000$). Descriptive statistics are reported in Table 2.

Table 2. Descriptive statistics for time to failure during passive falls to ±30°.

Condition	Mean Time to Failure (s)	SD	SE	Coefficient of variation
Short	1.128	0.245	0.055	0.218
Medium	1.368	0.284	0.063	0.207
Long	1.440	0.370	0.083	0.257

Time to failure did not vary significantly across trials within any of the three pendulum lengths. A repeated-measures analysis including both trial number and condition revealed no significant Condition × Trial interaction ($F(2, 57) = 0.015$, $p = 0.985$), indicating that performance remained stable across repetitions. This confirms that the observed differences between conditions were not driven by trial order or sequential variability. The distribution of trial-wise values is visualized in Figure 4. As expected, these findings clearly show that longer pendulums exhibit greater passive stability, taking longer to reach the ±30° threshold.

Figure 4. Time to failure for passive falls of absolute angle to 30° across pendulum conditions. Individual trial data are shown for short, medium, and long pendulums, displayed with horizontal jitter for clarity. Black squares indicate the group means, and error bars denote the standard error of the mean (±SE).

Study 2: Human Study of Balance

Time To Failure

As shown in Figure 5A, participants significantly improved their ability to maintain balance during the training phase with the medium length pendulum. Their average time to failure increased from 1.4 seconds at the beginning phase to 3.46 seconds at the end phase, based on the first and last 10% of training trials. This improvement was confirmed by a repeated-measures ANOVA, which revealed a significant main effect, $F(1, 1) = 15.518$, $p < 0.001$, $\omega^2 = 0.146$, indicating robust improvement. No significant interaction between phase and participant was found ($p = 0.573$), suggesting that the improvement trend was consistent across individuals. In contrast, during the testing phase, as observed in Figure 5B-D, performance did not follow the same trend seen during initial training and plateaued out.

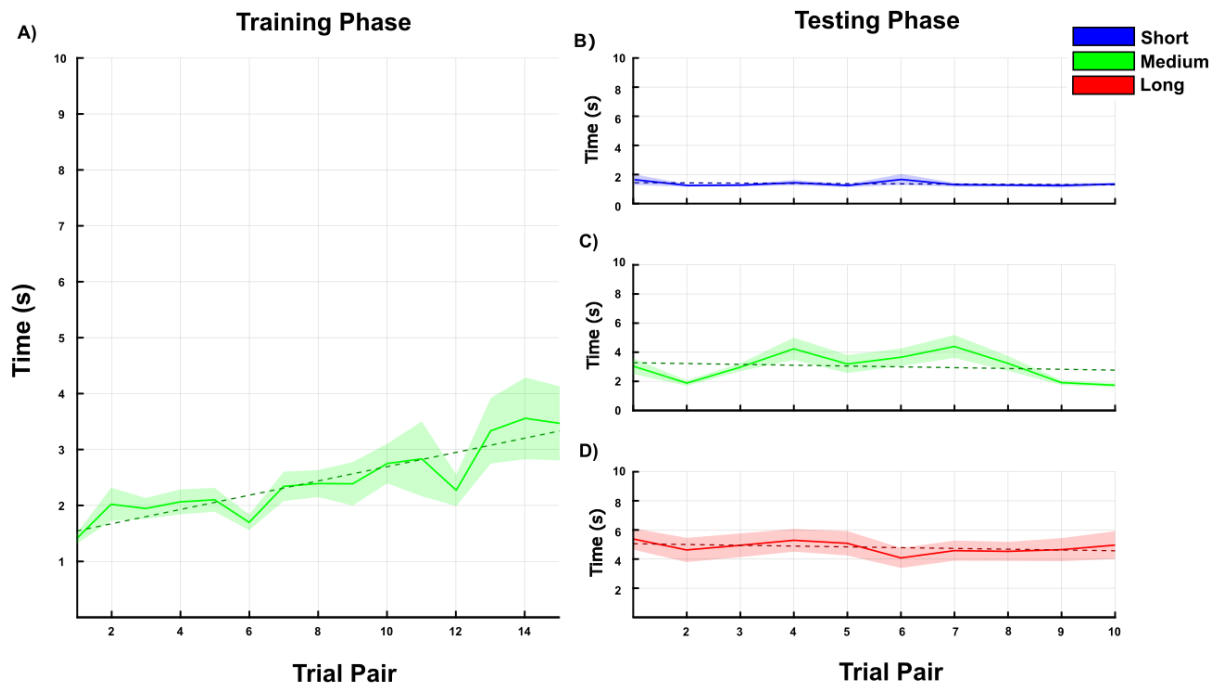

Figure 5. Time to failure across human participants and across trials. **A)** Trial times during the medium size pendulum training phase. **B)** Time to failure during the testing short pendulum condition. **C)** Time to failure during the testing medium pendulum condition. **D)** Time to failure during the testing long pendulum condition.

As shown in Figure 6A, participants' time to failure during the final 10% of testing trials increased significantly with pendulum length. The mean time to failure was 1.35 seconds for the short pendulum, 1.70 seconds for the medium pendulum, and 4.95 seconds for the long pendulum. A one-way ANOVA confirmed a significant effect of condition on time to failure ($F(2,66) = 23.69$, $p < 0.001$, $\omega^2 = 0.378$). Post-hoc comparisons revealed that participants balanced the long pendulum significantly longer than both the medium ($p < 0.001$) and short ($p < 0.001$) pendulums.

Group order (Group A vs. Group B) did not significantly affect performance ($F(1,66) = 2.56$, $p = 0.114$). However, descriptive trends suggested that Group B exhibited longer time to failure, particularly in the long pendulum condition (Group A: Mean = 4.00, Group B: Mean = 5.90), though this difference was not statistically significant ($p = 0.197$). See Figure 6B for further details.

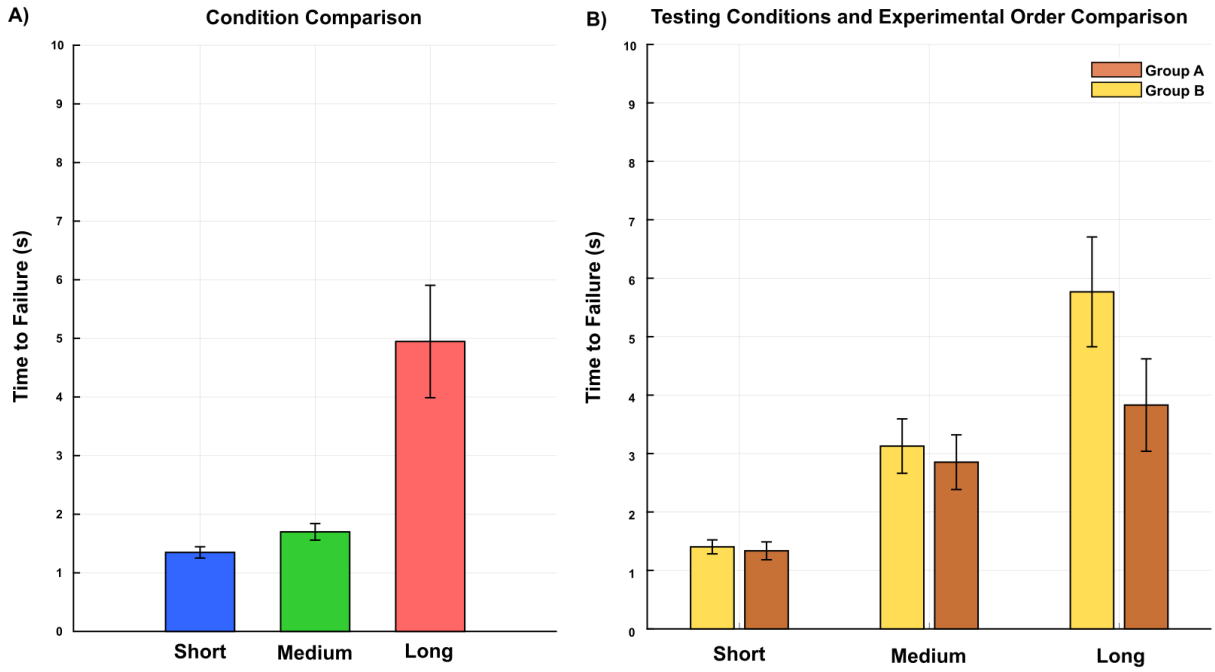

Figure 6. Time to failure across human participants during the last 10% of trials. **A)** Time to failure across each pendulum length condition. **B)** Between-subject comparison of mean time to failure for each pendulum length condition.

Peak Velocity

To better understand how participants adapted their control strategies across pendulum conditions, we examined peak encoder angular velocity for both the cart and pendulum during the final 10% of trials, when behavior had stabilized.

As seen in Figure 7A, peak cart velocity remained consistent across all three rod lengths. Regardless of whether participants were balancing the short, medium, or long pendulum, the maximum speed they applied to the cart converged on a similar value. Statistically, there was no main effect of condition, $F(2,22) = 0.063$, $p = 0.939$. The group means were tightly clustered, 61,209 ± 5,056 $deg \cdot s^{-1}$ for short, 64,038 ± 6,323 $deg \cdot s^{-1}$ for medium, and 59,830 ± 11,197 $deg \cdot s^{-1}$ for long. These findings suggest that, once stable control was achieved, participants adopted similar range of actuation effort, independent of the pendulum's length.

However, despite similar control inputs, the rod's responses diverged across conditions. Peak pendulum angular velocity varied systematically with rod length (see Figure 7B). A repeated-measures ANOVA revealed a main effect of condition, $F(2,22) = 5.486$, $p = 0.012$, with effect size $\omega^2 = 0.21$. Pendulum angular velocities were highest for the short

condition (1,599 ± 14 deg·s $^{-1}$), slightly lower for medium (1,561 ± 7 deg·s $^{-1}$), and lowest for long (1,123 ± 190 deg·s $^{-1}$). Although pairwise comparisons did not reach significance after Holm correction (p_s= 0.091 - 0.132), the observed trend remained robust and aligned with mechanical expectations: longer pendulums, owing to their greater inertia, exhibited slower responses to equivalent control inputs.

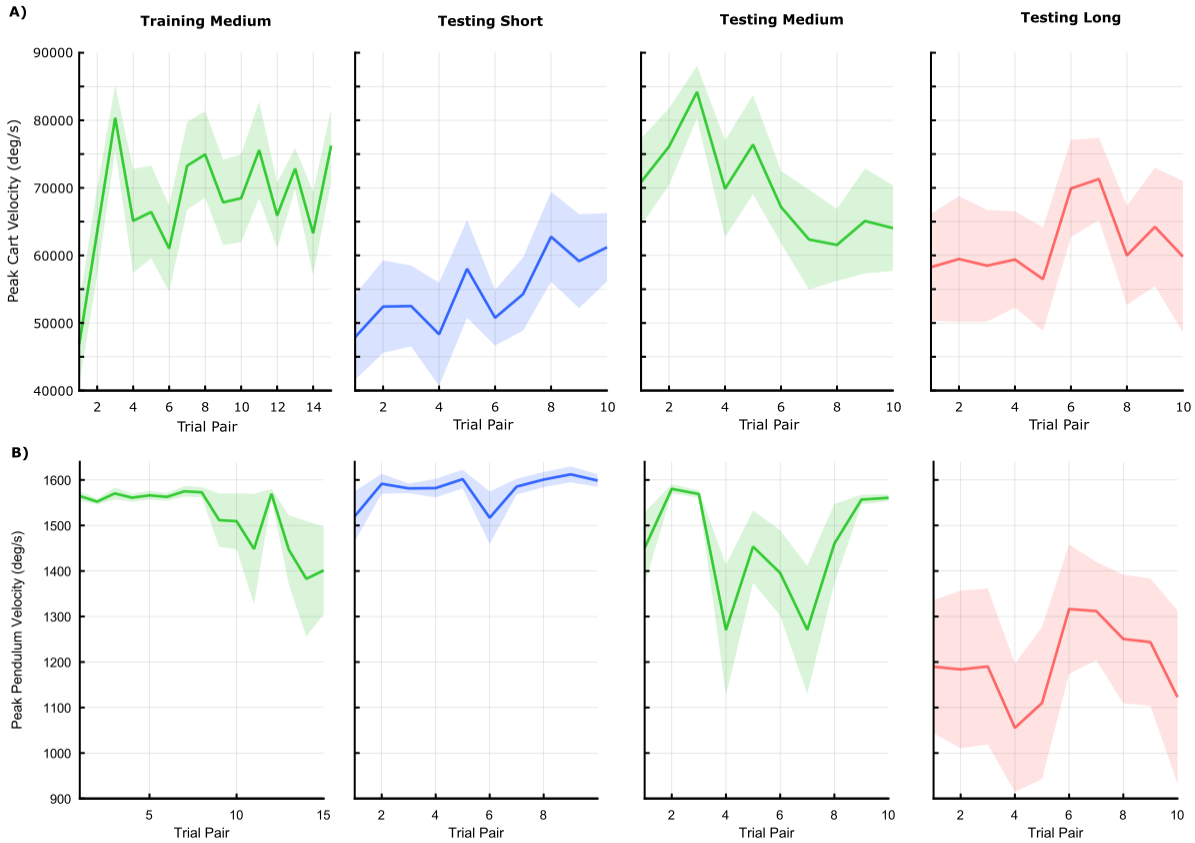

Figure 7. Peak angular velocities for the different pendulum length condition and experimental phase. **A)** Per trial-pair peak cart encoder angular velocities. The colored line represents the group mean, with the shaded band showing ±1 standard error (SE). The x-axis indicates the trial-pair index. Velocities are computed as absolute peak values (|deg·s $^{-1}$|). **B)** Per trial-pair peak pendulum encoder angular velocities. As in panel A, colored lines show the group mean, and shaded bands denote ±SE across participants.

To explore this further, we compared performance across phases within the medium condition, where both training and testing were available (Figure 7C-D). Cart encoder angular velocities were again similar across phases, $F(1,11) = 1.488$, $p = 0.248$ (72,582 ± 3,638 vs. 64,038 ± 6,323 deg·s $^{-1}$), but pendulum encoder angular velocities increased slightly at testing $F(1,11) = 4.843$, $p = 0.050$ (1,411 ± 67 vs. 1,561 ± 7 deg·s $^{-1}$).

Discussion (1033/1500)

Understanding how humans behave in real physical environments is a central question in motor control research. While most previous studies have used simplified, virtual tasks,

our study explores control in a physically unstable, real-world system. This is the manual balancing of inverted pendulums of three different lengths, with difficulty decreasing as length increases. We first investigate the passive dynamics of the pendulums and then assess the ability of human participants to balance them.

Comparative results: passive mechanics vs human control

Across both experiments, as expected, a consistent relationship emerged between the passive mechanical properties of the pendulum system and human performance during active balancing.

The passive characterization revealed that pendulum length substantially modulated the plant's intrinsic dynamics. As it is already well known, longer rods exhibited greater decay durations and lower dominant frequencies, whereas shorter rods decayed more rapidly and oscillated at higher frequencies. In the fall to either ±30° trials, the time to failure followed the same ordering, confirming that longer rods are inherently more stable under passive conditions. These differences affect controllability, with longer rods providing greater temporal margins for correction, while shorter rods demand faster and more precise intervention to maintain stability.

We note that static friction at the pivot must be overcome to initiate motion and is less consequential in longer pendulums, where larger restoring torques are available; therefore, stiction becomes proportionally more significant in shorter pendulums. This stiction factor would assist balancing of shorter pendulums, although this was not a significant factor in our experiments. An energy-based perspective helps explain the decay results: for the same angular range, longer pendulums store and exchange more energy, so even with comparable dissipation mechanisms, the longer rods take more time to settle. Conversely, shorter pendulums decay more quickly because the energy per cycle is smaller.

Human behavior during active balancing mirrored these mechanical constraints. Participants first trained on the medium pendulum, where performance improved over trials, as evidenced by an increase in time to failure. This indicates practice improved the control strategy for the medium rod. When subsequently tested on all three rods, performance did not improve further in any condition, but rather performance outcomes aligned with predictions based on the passive analysis: time to failure was highest for the long rod, intermediate for the trained medium rod, and lowest for the short rod. Thus, the intrinsic temporal dynamics of the plant imposed fundamental limits on controllability, even after initial practice had been experienced.

We found that the performance effect across pendulum lengths was not attributable to differences in movement speed. By the end of testing, peak cart encoder angular velocities had converged to comparable values across all three conditions, indicating that participants applied comparable maximum levels of actuation effort regardless of pendulum length. However, the response of the plant diverged: peak pendulum angular velocities were significantly higher in the short rod condition and lower in the long rod condition. This dissociation reveals that while participants behaved similarly across conditions, the mechanical consequences of those actions were governed by rod length.

Comparisons between training and testing on the medium rod further support the interpretation that practice resulted in refinement of coordination, rather than changes in movement speed. Peak cart velocities did not increase between training and testing phases.

These findings yield two key takeaway messages. First, with practice, individuals do not primarily learn to move faster, but rather to move more effectively, refining the timing, coordination, and structure of their control strategies to better suit the dynamics of the system. Second, as is well known, longer pendulums are easier to balance than shorter ones because their slower dynamics provide a larger temporal margin for error detection and correction, making the task inherently more forgiving and controllable.

Relation to previous work on physical pendulums

There have been numerous studies examining balancing of physical inverted pendulums (Loram and Lakie, 2002; Lakie et al., 2003; Cabrera and Milton, 2004). They have long been a model for studying human balance control, especially in tasks such as stick-balancing and cart-pendulum balancing, which closely mirror real-world balance (Yoshikawa et al., 2016).

A central theme in this literature is that there is time delayed feedback, which complicates balance control and strongly affects how human participants can perform balancing tasks. This leads to reaction time delays, which are crucial for balancing performance, and longer pendulums tend to result in longer times to failure (Kovacs and Insperger, 2022). Additionally, previous research has highlighted the role of both active feedback and intrinsic passive stiffness in balance maintenance, which aligns with our observation of the interplay between active and passive dynamics in balancing (Loram and Lakie, 2002; Lakie et al., 2003).

Intermittent feedback control, which alternates between active corrections and passive stabilization, has been proposed to enhance stability, particularly in more complex systems, supporting the conclusion that longer pendulums require more sophisticated feedback strategies (Yoshikawa et al., 2016). Studies have shown that intermittent corrections are crucial for maintaining stability, with one example being the instability of the upright fixed point in time-delayed systems (Milton et al., 2009). Additionally, skilled stick balancing has been shown to follow a Lévy flight pattern, characterized by bursts of corrective movement and periods of inactivity (Cabrera and Milton, 2004).

Interestingly, consistent manual adjustments across pendulum configurations suggest fixed temporal constraints for balance control, a pattern we observed in the increased complexity of balancing longer pendulums (Loram and Lakie, 2002). Our findings support this concept, showing that longer pendulums lead to more variation in time to failure. Reaction time delays are known to influence balancing performance, as reflected in our study, where longer pendulums corresponded with longer times to failure.

Future work

The preliminary results from the current experiments could provide quantitative data for future research to extend the analysis through computational modelling of real-time

control that integrates human biological constraints. Building on our previous dual linear-quadratic regulator (LQR) framework for this apparatus (Alvarez Hidalgo and Howard, 2022, 2024), forthcoming models will incorporate sensory delays, signal-dependent noise, static friction, and actuation limits, all of which are factors known to influence motor planning and feedback regulation in unstable tasks. Such models may account for key empirical findings observed here, including the near invariance of peak cart velocities across conditions.

Disclosures

The authors declare that they have no financial, personal, or professional conflicts of interest that may have influenced the content of this paper.

Author Contributions

LAH and ISH conceived the study. LAH implemented the study, conducted data collection, and performed data analysis. The initial draft of the manuscript was written by LAH. All authors, LAH and ISH, reviewed and edited the manuscript.

References

Alvarez Hidalgo L, Howard IS (2022) Gain scheduling for state space control of a dual-mode inverted pendulum. In: 2022 International Conference on System Science and Engineering (ICSSE), pp 039–046. IEEE.

Alvarez Hidalgo L, Howard IS (2024) Dual Mode Control of an Inverted Pendulum: Design, Analysis and Experimental Evaluation. Adv Sci Technol Eng Syst J 8:120–143.

Burdet E, Osu R, Franklin DW, Milner TE, Kawato M (2001) The central nervous system stabilizes unstable dynamics by learning optimal impedance. Nature 414:446–449.

Cabrera JL, Milton JG (2004) Human stick balancing: Tuning Lèvy flights to improve balance control. Chaos Interdiscip J Nonlinear Sci 14:691–698.

Franklin DW, Wolpert DM (2011) Computational mechanisms of sensorimotor control. Neuron 72:425–442.

Gawthrop PJ, Wang L (2006) Intermittent predictive control of an inverted pendulum. Control Eng Pract 14:1347–1356.

Howard I, Ford C, Cangelosi A, Franklin D (2017) Active lead-in variability affects motor memory formation and slows motor learning. Sci Rep 7:7806.

Howard I, Ingram J, Wolpert D (2009) A modular planar robotic manipulandum with end-point torque control. J Neurosci Methods 181:199–211.

Howard IS, Ingram JN, Franklin DW, Wolpert DM (2012) Gone in 0.6 Seconds: The Encoding of Motor Memories Depends on Recent Sensorimotor States. J Neurosci 32:12756–12768.

Howard IS, Wolpert DM, Franklin DW (2013) The effect of contextual cues on the encoding of motor memories. J Neurophysiol 109:2632–2644.

Kovacs BA, Insperger T (2022) Virtual stick balancing: skill development in Newtonian and Aristotelian dynamics. J R Soc Interface 19:20210854.

Krakauer JW, Mazzoni P (2011) Human sensorimotor learning: Adaptation, skill, and beyond. Curr Opin Neurobiol 21:636–644.

Lakie M, Caplan N, Loram ID (2003) Human balancing of an inverted pendulum with a compliant linkage: neural control by anticipatory intermittent bias. J Physiol 551:357–370.

Liu D, Todorov E (2007) Evidence for the Flexible Sensorimotor Strategies Predicted by Optimal Feedback Control. J Neurosci 27:9354–9368.

Loram ID, Lakie M (2002) Human balancing of an inverted pendulum: position control by small, ballistic-like, throw and catch movements. J Physiol 540:1111–1124.

Mehta B, Schaal S (2002) Forward models in visuomotor control. J Neurophysiol 88:942–953.

Milner TE, Franklin DW (2005) Impedance control and internal model use during the initial stage of adaptation to novel dynamics in humans. J Physiol 567:651–664.

Milton J, Cabrera JL, Ohira T, Tajima S, Tonosaki Y, Eurich CW, Campbell SA (2009) The time-delayed inverted pendulum: Implications for human balance control. Chaos Interdiscip J Nonlinear Sci 19:026110.

Oldfield RC (1971) The assessment and analysis of handedness: The Edinburgh inventory. Neuropsychologia 9:97–113.

Scott SH (2004) Optimal feedback control and the neural basis of volitional motor control. Nat Rev Neurosci 5:532–546.

Shadmehr R, Smith MA, Krakauer JW (2010) Error correction, sensory prediction, and adaptation in motor control. Annu Rev Neurosci 33:89–108.

Taylor JA, Ivry RB (2012) The role of strategies in motor learning. Ann N Y Acad Sci 1251:1–12.

Wolpert DM, Diedrichsen J, Flanagan JR (2011) Principles of sensorimotor learning. Nat Rev Neurosci 12:739–751.

Yoshikawa N, Suzuki Y, Kiyono K, Nomura T (2016) Intermittent Feedback-Control Strategy for Stabilizing Inverted Pendulum on Manually Controlled Cart as Analogy to Human Stick Balancing. Front Comput Neurosci 10.